LATTICE THERMAL CONDUCTIVITY OF TRANSITION METAL DICHALCOGENIDES

Alexej Alexeev*, Anna Krivosheeva, Viktor Shaposhnikov, Viktor Borisenko

Belarusian State University of Informatics and Radioelectronics, Minsk, Belarus

*e-mail: lucky.alexey94@gmail.com

Abstract. Ab initio simulation of phonon spectra and lattice thermal conductivity of monomolecular layers of transition metal dichalcogenides is performed. Size and temperature dependence of lattice thermal conductivity are analyzed and the difference between transition metal dichalcogenides is explained.
Keywords: dichalcogenide, phonon, thermal conductivity, transition metal, monolayer

1. Introduction
Monomolecular layers (ML) of transition metal dichalcogenides (TMD) are two-dimensional graphene-like materials which have great perspectives in electronics and optoelectronics due to the fact that they are direct-gap semiconductors with a relevant band gap [1]. Moreover, the TMD monolayers have perspectives in spintronics and valleytronics [2]. An individual ML of TMD can be easily synthesized from bulk TMD [3] because bulk TMD is a layered crystal with weak interlayer van der Waals bonds and strong intralayer forces. Besides they can be fabricated by means of the bottom-up method like a chemical vapor deposition [4].

In the most stable H-phase [5], one ML has a three-layer sandwich structure Chal–Me–Chal (Chal = S, Se, Te; Me = Mo, W) with the space symmetry of $P\bar{6}m2$ (No. 187). In this H-phase a metal atom is located in the trigonal prism formed by chalcogen atoms. The H-phase is not the most stable phase for a monolayer WTe_2 but it is stable enough [5] that was also confirmed by our theoretical results for its phonon spectrum.

In recent years, a lot of attention is paid to exploration of monolayer TMDs. In this work, we deal with phonon properties, in particular we carried out the ab initio investigation of lattice thermal conductivity. There are some contradictory experimental measurements of lattice thermal conductivity of monolayer TMDs [6–9], whereas this property is very important for the applications in integrated circuits or thermoelectric devices. Because of this, the theoretical investigations on this issue are needed.

2. Computational method and details
The lattices optimization and calculations of harmonic and cubic anharmonic force constants (FC) were performed through the use of the density functional theory (DFT) [10] within local density approximation (LDA) [10] with the help of Vienna Ab initio Simulation Package (VASP) [11]. The cutoff energy in all the simulations was set to 320 eV. The unit cell of monolayer TMD is a hexagonal cell with three atoms (one metal and two chalcogen atoms), an additional vacuum layer being between monomolecular layers. The vacuum layer thickness was chosen to be 12 Å.

For force constant calculations, the finite displacement method was applied [12]. We used 4×4×1 supercell and 6×6×1 k-mesh sampling for the harmonic-force-constant

calculations and $2\times2\times1$ supercell and $12\times12\times1$ k-mesh sampling for the anharmonic-cubic-force-constant calculations. The harmonic force constants were used for obtaining the dynamic matrix by the *phonopy package* [13] for the calculations of phonon spectrum and density of phonon states (phonon DOS). The anharmonic-cubic-force-constants were used for calculations of phonon relaxation time within the *phono3py package* by using the technique described in Ref. [14]. For boundary scattering (BS), we used a very simple model provided by *phono3py package* [14]. Isotope scattering (IS) with natural isotope distribution for each element is described by the second-order perturbation theory [15]. The total phonon scattering rate $1/\tau_\lambda$ is defined as the sum of scattering rates of both scattering mechanisms. The phonon spectrum and total scattering rate were used for calculation of the lattice thermal conductivity tensor κ within the single mode relaxation time approximation (SMRTA) [14].

$$\kappa = \frac{1}{NV_0}\sum_\lambda C_\lambda \vec{v}_\lambda \otimes \vec{v}_\lambda \tau_\lambda, \tag{1}$$

where N is the number of unit cells in the crystal, V_0 is the unit cell volume, λ is the phonon mode index that includes band index and wave vector, C_λ is the heat capacity of the λ phonon mode (its contribution to the total heat capacity), and $\vec{v}_\lambda$ is the group velocity of phonon λ. The unit cell thickness for calculation of V_0 value is chosen as the half of appropriate pre-calculated theoretical lattice constant of bulk counterpart. The thickness is given in Table 1.

Table 1. Monolayer thickness used for calculating V_0 values

ML TMD	ML MoS$_2$	ML MoSe$_2$	ML MoTe$_2$	ML WS$_2$	ML WSe$_2$	ML WTe$_2$
Thickness, Å	6.02	6.36	6.07	6.42	6.88	6.91

The full solution of linearized Boltzmann transport equation should give the close but larger values of lattice thermal conductivity [16], so the presented results must be considered as the lower limits. The LO-TO splitting from monolayer TMDs is small [17] and generally is not taken into account. In this work, we also neglect LO-TO splitting.

3. Results and Discussion

The calculated phonon spectra and phonon density of states for monolayer TMDs are presented in Fig. 1. The phonon spectra are in a good agreement with previous results [17–20]. The phonon spectrum of monolayer WTe$_2$ does not have an imaginary mode that means the stability of considered H-phase. There are three notes from Fig. 1 needed for lattice thermal conductivity analysis.

Note 1. The group velocities $\vec{v}_\lambda$ of acoustic modes decreases with increasing molecular mass of the compounds, so that monolayer WTe$_2$ has the lowest values and monolayer MoS$_2$ has the biggest values of $\vec{v}_\lambda$ of acoustic modes; $\vec{v}_\lambda$ values explicitly being present in Equation 1 for κ value.

Note 2. In the low frequency range, the monolayer WTe$_2$ has the largest number of phonon states, as seen from phonon DOS plots. This is also a consequence from the largest value of molecular mass; the larger mass, the lower phonon mode frequency, so the identical (from different monolayer TMDs) phonon modes lie in the lower frequency range. Because of that, there is the steepest rise on the temperature dependence of the phonon number for monolayer WTe$_2$. This affects the lattice thermal conductivity through the summation over all the phonon modes with Cλ values as coefficients in Equation 1. Thus the monolayer MoTe$_2$ has slightly smaller slope and the monolayer MoS$_2$ has the smallest slope of temperature dependence on the phonon number.
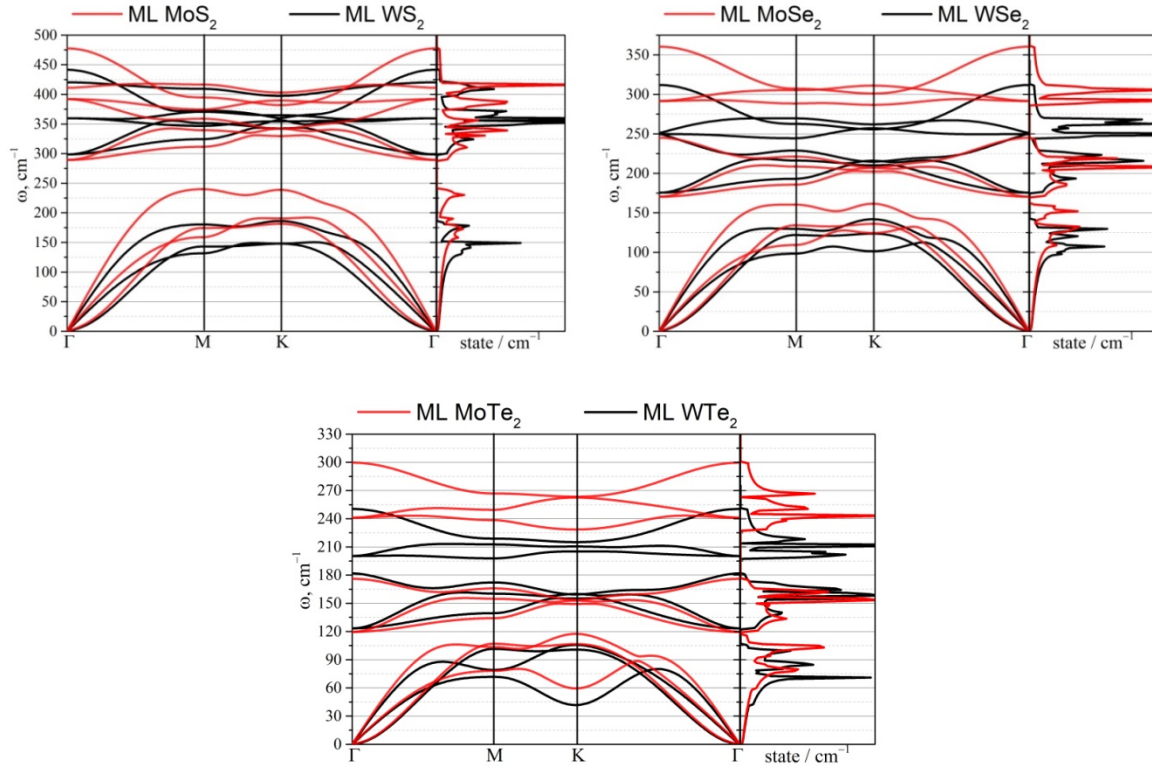
Fig. 1. Phonon spectra and density of phonon states for monolayer TMDs

Note 3. The monolayer WS_2 has remarkable large value of the gap $\Delta\omega_{a-o}$ between acoustic and optical phonon modes. The $\Delta\omega_{a-o}$ value affects the lattice thermal conductivity because of the energy conservation law in phonon-phonon scattering processes. The calculated xx- and yy-components of the lattice thermal conductivity tensor for monolayer TMDs are equal to each other. Other calculated components of the tensor are equal to zero. In this article, we assign by κ an xx-component of lattice thermal conductivity tensor.

Figure 2 shows the dependencies of κ on the sample size L at room temperature for monolayer TMDs. This size dependence of κ only appears because of boundary scattering and L value is presented in the model only as a parameter. Figure 3 shows the κ dependencies on temperature T with 1 μm sample size L. The calculated lattice thermal conductivity of monolayer TMDs is in agreement with previous results [16, 21]. For the detail analysis, the temperature dependence of κ without IS and BS is presented in Fig. 4.
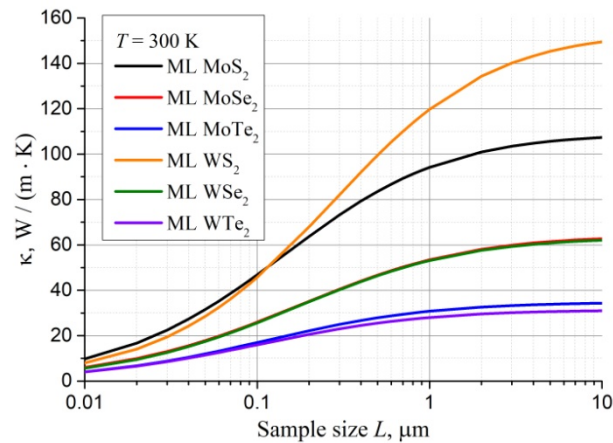

Fig. 2. Dependence of lattice thermal conductivity κ on sample size L at room temperature for monolayer TMDs (diselenides have very close lying curves)
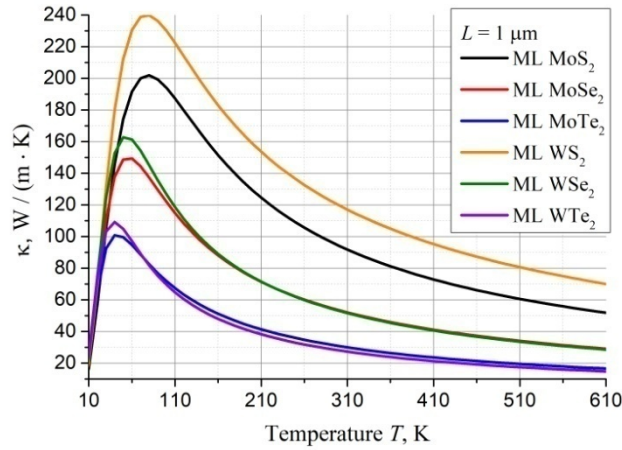
Fig. 3. Dependency of lattice thermal conductivity κ on temperature *T* for monolayer TMDs with sample size 1 μm
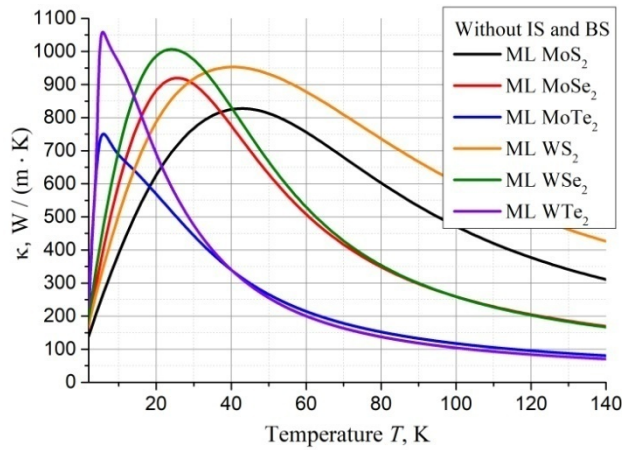

Fig. 4. Dependence of lattice thermal conductivity κ on temperature *T* for monolayer TMDs without isotope and boundary scattering

With increasing temperature from 0 K, the heat carriers (phonons) appear, but there are no any scattering mechanisms at such temperatures in the case shown in Fig. 4. This means that κ tends to infinity. Monolayer WTe$_2$ has the steepest rise and monolayer MoS$_2$ has the smallest slope on temperature dependence of κ in the low temperature range, because of the reason specified above in Note 2. Then, κ value decreases because of inclusion of phonon-phonon scattering and thus, there appears a peak on the temperature dependence. The temperatures that correspond to the maximum κ values for materials with different metals and the same chalcogen are similar, because of the similar phonon spectra and, in particular, similar low frequency range. The larger phonon number in the low frequency range, the larger the number of possible phonon-phonon scatterings; thus, ditellurides reach the maximums at smaller temperatures than diselenides, and diselenides reach maximum at smaller temperatures than disulfides. The difference between the maximum of κ values is due to the difference between steepness of the κ rise that was explained above.

The ditellurides have notable bend in the after-peak range. This is explained by a sharp rise of the number of phonons, associated with the first peak on the phonon DOS plot, which occurs at the after-peak temperatures.

The values of κ of different monolayer TMDs at large temperatures can be explained by $\vec{v}_\lambda$ values and the selection rules for phonon-phonon scattering processes. We estimate

selection rules (energy conservation) contribution in the following way. One of the most important phonon-phonon scattering channels is the annihilation of two acoustic phonon modes into one optical one [22–23]. For estimating the contribution of such processes we calculated half the frequency at the bottom of optical modes ($\omega_{\text{optical bottom}} / 2 = (\omega_{\text{acoustic top}} + \Delta\omega_{\text{a-o}}) / 2$) and the fraction of this value from the acoustic frequency range $((1 + \Delta\omega_{\text{a-o}} / \omega_{\text{acoustic top}}) / 2)$. This value, as well as all the necessary frequencies, and κ values at room temperature are presented in Table 2.

Table 2. Calculated κ values at 300 K, frequencies characterizing the spectrum and the proposed estimation of selection rules contribution for monolayer TMDs

	ML MoS$_2$	ML MoSe$_2$	ML MoTe$_2$	ML WS$_2$	ML WSe$_2$	ML WTe$_2$
κ with $L = 1$ µm, W / (m · K)	94.21	53.46	30.79	119.78	53.07	28.06
κ without IS and BI, W / (m · K)	126.70	71.98	36.37	189.44	70.25	31.31
$\omega_{\text{acoustic top}}$, cm^{-1}	230.80	161.43	117.39	186.19	141.90	105.74
$\Delta\omega_{\text{a-o}}$, cm^{-1}	49.44	8.84	2.14	112.40	33.60	17.65
$\omega_{\text{optical bottom}}$, cm^{-1}	280.24	170.27	119.53	298.59	175.50	123.39
Estimation of selection rules contribution, %	60.7	52.7	50.9	80.2	61.8	58.4

The larger value of proposed estimation means the smaller number of permitted phonon-phonon scattering processes. Monolayer WS$_2$ has the remarkable large value of this estimation because of large $\Delta\omega$a-o value (see Note 3 above). Thus, monolayer WS$_2$ has the larger value of κ despite of the fact that monolayer MoS$_2$ has larger $\vec{v}_\lambda$ values (see Note 1 above). For diselenides and ditellurides the difference between selection rules contribution and between $\vec{v}_\lambda$ balances each other, so that monolayer MoSe$_2$ and WSe$_2$ have similar κ values and monolayer MoTe$_2$ and WTe$_2$ have also similar κ values. Ditellurides have smaller κ values than diselenides; and diselenides have smaller κ values than disulfides mainly due to the difference between $\vec{v}_\lambda$ (see Note 1 above). Thus, it is possible to predict comparative values of κ for the crystals with a same crystal structure by using only phonon spectra (by calculation of group velocities and proposed estimation) without anharmonic calculation.

In Figure 5 the κ dependence on temperature for 1 µm sample size L without IS is presented. When BS is taken into account, the scattering is presented starting at 0 K, thus, the κ rise is less steep. The steepness is determined by neglecting phonon-phonon scattering mechanisms and, as a result, is balanced by the differences between the number of heat carriers and between $\vec{v}_\lambda$ values (see Notes 1 and 2 above). As a consequence, the steepness of κ rise for different monolayer TMDs has a very similar value. For the same reasons, in the case of temperature dependence without BS, the temperatures corresponding to the maximum κ values have smaller values for ditellurides and larger values for disulfides. These temperatures have larger values than in the case without BS due to the fact that phonon-phonon scattering has lesser influence (comparable with the BS magnitude).

When the sample size decreases (see Fig. 2) BS dominates. All monolayer TMDs have close κ values that are again determined by balance of differences between number of heat carriers and between $\vec{v}_\lambda$ values. When IS is taken into account (see Fig. 3) the similarities in peaks in Fig. 5 disappear due to the different natural distributions of different elements. At that all κ values decrease that obviously follows from the existence of additional scattering mechanism.
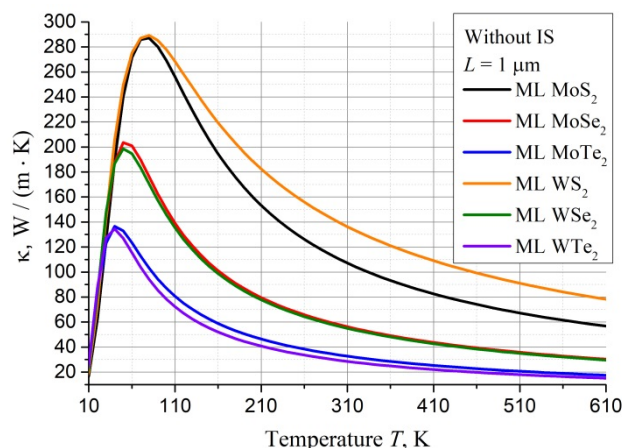
Fig. 5. Dependencies of lattice thermal conductivity κ on temperature for monolayer TMDs with sample size 1 μm without isotope scattering

4. Conclusions

The results of ab initio calculations of lattice thermal conductivities of monolayer transition metal dichalcogenides are presented and analyzed. The calculated values of lattice thermal conductivities are close to the values of materials commonly used in microelectronics (Si, Ge and GaAs). Because of the large group velocity and forbiddance of many phonon-phonon scattering processes, monolayer WS_2 has the largest κ value and because of small group velocity, ditellurides have the smallest κ value among the crystals studied. These results can be used for better understanding phonon transport mechanisms and for searching new materials and ways of their properties modifications. For estimating the contribution of selecting rules, the parameter $\omega_{optical\ bottom} / \omega_{acustic\ top} / 2$ is proposed. It takes into account the selection rules into phonon-phonon scattering process with two acoustic and one optical phonon.

    The comparative values of lattice thermal conductivity of the crystals with a same crystal structure can be estimated by using the phonon spectra even without anharmonic calculations. Generally, it is expected that smaller lattice thermal conductivity, which is required for thermoelectric applications, will be observed in the compounds with larger molecular mass (as a consequence, smaller group velocity) and smaller parameter that are proposed in this work. If there is no gap between acoustic and optical modes, the parameter has the value less than 50 %. For example, Bi_2Te_3 (commonly used in thermoelectric devices material with $\kappa = 1.20$ W/(m·K)) has large molecular mass and does not have acoustic-optical gap.

References

[1] K.F. Mak, C. Lee, J. Hone, J. Shan, T.F. Heinz, Atomically thin MoS_2: a new direct-gap semiconductor // *Phys. Rev. Lett.* **105(13)** (2010) 136805.

[2] Q.H. Wang, K. Kalantar-Zadeh, A. Kis, J.N. Coleman, M.S. Strano, Electronics and optoelectronics of two-dimensional transition metal dichalcogenides // *Nature Nanotech.* **7(11)** (2012) 699.

[3] K.S. Novoselov, D. Jiang, F. Schedin, T.J. Booth, V.V. Khotkevich, S.V. Morozov, A.K. Geim, Two-dimensional atomic crystals // *Proc. Nat. Acad. Sci. U.S.A.* **102(30)** (2005)10451.

[4] Y. Yu, C. Li, Y. Liu, L. Su, Y. Zhang, L. Cao, Controlled scalable synthesis of uniform, high-quality monolayer and few-layer MoS_2 films // *Scientific Reports* **3(1866)** (2013) 1.

[5] K.C. Santosh, C. Zhang, S. Hong, R.M. Wallace, K. Cho, Phase stability of transition metal dichalcogenide by competing ligand field stabilization and charge density wave // *2D Materials* **2(3)** (2015) 035019.

[6] R. Yan, J.R. Simpson, S. Bertolazzi, J. Brivio, M. Watson, X. Wu, A. Kis, T. Luo, A.R.H. Hight, H.C. Xing, Thermal conductivity of monolayer molybdenum disulfide obtained from temperature-dependent Raman spectroscopy // *ACS Nano* **8(1)** (2014) 986.

[7] S. Sahoo, A.P. Gaur, M. Ahmadi, M.J.F. Guinel, R.S. Katiyar, Temperature-dependent Raman studies and thermal conductivity of few-layer MoS_2 // *J. Phys. Chem. C* **117(17)** (2013) 9042.

[8] A. Taube, J. Judek, A. Łapińska, M. Zdrojek, Temperature-dependent thermal properties of supported MoS_2 monolayers // *ACS Appl. Mater. Interfaces* **7(9)** (2015) 5061.

[9] I. Jo, M.T. Pettes, E. Ou, W. Wu, L. Shi, Basal-plane thermal conductivity of few-layer molybdenum disulfide // *Appl. Phys. Lett.* **104(20)** (2014) 201902.

[10] M.C. Payne, M.P. Teter, D.C. Allan, T.A. Arias, J.D. Joannopoulos, Iterative minimization techniques for ab initio total-energy calculations: molecular dynamics and conjugate gradients // *Rev. Mod. Phys.* **64(4)** (1992) 1045.

[11] G. Kresse, F. Furthmüller, Efficiency of ab-initio total energy calculations for metals and semiconductors using a plane-wave basis set // *Comput. Mater. Sci.* **6(1)** (1996) 15.

[12] L. Chaput, A. Togo, I. Tanaka, G. Hug, Phonon-phonon interactions in transition metals // *Phys. Rev. B* **84(9)** (2011) 094302.

[13] A. Togo, I. Tanaka, First principles phonon calculations in materials science // *Scripta Materialia* **108** (2015) 1.

[14] A. Togo, L. Chaput, I. Tanaka, Distributions of phonon lifetimes in Brillouin zones // *Phys. Rev. B* **91(9)** (2015) 094306.

[15] S.I. Tamura, Isotope scattering of dispersive phonons in Ge // *Phys. Rev. B* **27(2)** (1983) 858.

[16] X. Gu, R. Yang, Phonon transport in single-layer transition metal dichalcogenides: A first-principles study // *Appl. Phys. Lett.* **105(13)** (2014) 131903.

[17] A. Molina-Sanchez, L. Wirtz, Phonons in single-layer and few-layer MoS_2 and WS_2 // *Phys. Rev. B* **84(15)** (2011) 155413.

[18] C. Ataca, M. Topsakal, E. Akturk, S. Ciraci, A comparative study of lattice dynamics of three-and two-dimensional MoS_2 // *J. Phys. Chem. C* **115(33)** (2011) 16354.

[19] M. Kan, H.G. Nam, Y.H. Lee, Q. Sun, Phase stability and Raman vibration of the molybdenum ditelluride ($MoTe_2$) monolayer // *Phys. Chem. Chem. Phys.* **17(22)** (2015) 14866.

[20] H. Guo, T. Yang, M. Yamamoto, L. Zhou, R. Ishikawa, K. Ueno, R. Saito, Double resonance Raman modes in monolayer and few-layer $MoTe_2$ // *Phys. Rev. B* **91(20)** (2015) 205415.

[21] W. Li, J. Carrete, N. Mingo, Thermal conductivity and phonon linewidths of monolayer MoS_2 from first principles // *Appl. Phys. Lett.* **103(25)** (2013) 253103.

[22] C. Kittel, *Introduction to Solid State Physics* (Wiley, 2005).

[23] L. Lindsay, D.A. Broido, T.L. Reinecke, First-principles determination of ultrahigh thermal conductivity of boron arsenide: a competitor for diamond // *Phys. Rev. Lett.* **111(2)** (2013) 025901.